Impact of ^{68}Ga-FAPI PET/CT Imaging on the Therapeutic Management of Primary and Recurrent Pancreatic Ductal Adenocarcinomas

Manuel Röhrich[1], Patrick Naumann[2–4], Frederik L. Giesel[1,5], Peter L. Choyke[6], Fabian Staudinger[1], Annika Wefers[7,8], Dawn P. Liew[1], Clemens Kratochwil[1], Hendrik Rathke[1], Jakob Liermann[2–4], Klaus Herfarth[2–4], Dirk Jäger[9,10], Jürgen Debus[2–5,11,12], Uwe Haberkorn[1,5,13,14], Matthias Lang*[7,15], Stefan A. Koerber*[2–4]

[1]Department of Nuclear Medicine, Heidelberg University Hospital, Heidelberg, Germany; [2]Department of Radiation Oncology, Heidelberg University Hospital, Heidelberg, Germany; [3]National Center for Tumor diseases (NCT), Heidelberg, Germany; [4]Heidelberg Institute of Radiation Oncology (HIRO), Heidelberg, Germany; [5]German Cancer Consortium (DKTK), partner site Heidelberg, Germany; [6]Molecular Imaging Program, Center for Cancer Research, National Cancer Institute, National Institutes of Health, Bethesda, Maryland; [7]Department of Neuropathology, Institute of Pathology, University Hospital Heidelberg, Heidelberg, Germany; [8]Clinical Cooperation Unit Neuropathology, German Consortium for Translational Cancer Research (DKTK), German Cancer Research Center (DKFZ), Heidelberg, Germany; [9]Department of Medical Oncology and Internal Medicine Virgin Islands, National Center for Tumor Diseases, University Hospital Heidelberg, Germany; [10]Clinical Cooperation Unit Applied Tumor Immunity, German Cancer Research Center (DKFZ), Heidelberg, Germany; [11]Heidelberg Ion-Beam Therapy Center (HIT), Department of Radiation Oncology, Heidelberg University Hospital, Heidelberg, Germany; [12]Clinical Cooperation Unit Radiation Oncology, German Cancer Research Center (DKFZ), Heidelberg, Germany; [13]Clinical Cooperation Unit, Department of Nuclear Medicine, German Cancer Research Center (DKFZ), Heidelberg, Germany; [14]Translational Lung Research Center Heidelberg, Member of the German Center for Lung Research DZL, Heidelberg, Germany; and [15]Department of Surgery, Heidelberg University Hospital, Heidelberg, Germany

Pancreatic ductal carcinoma (PDAC) is a highly lethal cancer, and early detection and accurate staging are critical to prolonging survival. PDAC typically has a prominent stroma including cancer-associated fibroblasts that express fibroblast activation protein (FAP). FAP is a new target molecule for PET imaging of various tumors. In this retrospective study, we describe the clinical impact of PET/CT imaging using ^{68}Ga-labeled FAP-inhibitors (^{68}Ga-FAPI PET/CT) in 19 patients with PDAC (7 primary, 12 progressive/recurrent). **Methods:** All patients underwent contrast-enhanced CT (ceCT) for TNM staging before ^{68}Ga-FAPI PET/CT imaging. PET scans were acquired 60 min after administration of 150–250 MBq of ^{68}Ga-labeled FAP-specific tracers. To characterize ^{68}Ga-FAPI uptake over time, additional scans after 10 or 180 min were acquired in 6 patients. SUV_{max} and SUV_{mean} values of PDAC manifestations and healthy organs were analyzed. The tumor burden according to ^{68}Ga-FAPI PET/CT was compared with TNM staging based on ceCT and changes in oncologic management were recorded. **Results:** Compared with ceCT, ^{68}Ga-FAPI PET/CT results led to changes in TNM staging in 10 of 19 patients. Eight of 12 patients with recurrent/progressive disease were upstaged, 1 was downstaged, and 3 had no change. In newly diagnosed PDAC, 1 of 7 patients was upstaged, and the staging of 6 patients did not change. Changes in oncologic management occurred in 7 patients. Markedly elevated uptake of ^{68}Ga-FAPI in PDAC manifestations after 1 h was seen in most cases. Differentiation from pancreatitis based on static imaging 1 h after injection was challenging. With respect to imaging after multiple time points, PDAC and pancreatitis showed a trend for differential uptake kinetics. **Conclusion:** ^{68}Ga-FAPI PET/CT led to restaging in half of the patients with PDAC and most patients with recurrent disease compared with standard of care imaging. The clinical value of ^{68}Ga-FAPI PET/CT should be further investigated.

Key Words: fibroblast activation protein; FAP; pancreatic ductal adenocarcinoma; PDAC; PET; TNM; staging

J Nucl Med 2021; 62:779–786
DOI: 10.2967/jnumed.120.253062

Pancreatic ductal adenocarcinoma (PDAC) is one of the most aggressive types of cancer, with a dismal 5-year survival rate of less than 10% (*1*). Optimal imaging of PDAC is crucial for accurate initial staging and selection of the primary therapy as well as for follow-up examinations to accurately detect local recurrence or metastatic spread as early and as completely as possible.

Standard-of-care imaging techniques for PDAC include transabdominal ultrasonography (*2*), CT (*3*), MRI (*4,5*), and endoscopic ultrasonography (*6*), with contrast-enhanced CT (ceCT) considered the gold standard for TNM staging in preoperative and follow-up settings (*7,8*). PET with ^{18}F-FDG is not part of the clinical routine, but is sensitive for initial TNM staging (*9*), evaluation of treatment response (*10*), and detection of recurrence (*11*). Furthermore, ^{18}F-FDG PET/CT imaging parameters may predict treatment efficacy and clinical outcome for PDAC (*12*). However, ^{18}F-FDG PET/CT is clearly not an ideal imaging agent for PDAC due to its variable detection of metastatic lymph nodes (*13*) and possible false-positive findings in inflammation (*14*).

Histologically, PDAC is characterized by its prominent desmoplastic stroma (*15,16*). In general, tumor stroma is composed of

Received Jul. 8, 2020; revision accepted Sep. 29, 2020.
For correspondence or reprints contact: Manuel Röhrich, Department of Nuclear Medicine, University Hospital Heidelberg, Im Neuenheimer Feld 400 69120 Heidelberg, Germany.
E-mail: manuel.roehrich@med.uni-heidelberg.de
*Contributed equally to this work.
Published online Oct. 23, 2020.

extracellular matrix proteins and specialized connective-tissue cells, including activated cancer-associated fibroblasts (CAFs) (*17,18*). CAFs in PDAC are derived from pancreatic stellate cells (*19*) and transform their tumor-promoting biologic properties through crosstalk with neoplastic cells (*19,20*). CAFs are thought to promote tumor growth, invasion, metastasis, and therapy resistance both in PDAC (*18,21*) and in other tumor entities (*22*). CAFs—in contrast to normal fibroblasts—express fibroblast activation protein (FAP) on their surface (*23*). FAP is a type II membrane-bound glycoprotein with dipeptidyl peptidase and endopeptidase activity (*24*). FAP is a promising new target molecule for PET imaging of various epithelial tumors, among them PDAC (*25–28*). Biologically, the application of PET/CT using radioactive labeled FAP-inhibitors (FAPI PET/CT) in PDAC is of special interest as this new imaging modality depicts tumor-stroma interaction, which is crucial for the tumorigenesis of PDAC and cannot be visualized by morphologic or metabolic imaging. Although previous studies have included single cases of PDAC (*27,29*), the clinical value of FAPI PET for PDAC has not yet been systematically investigated.

The purpose of this investigation is to explore the clinical impact (TNM staging) of ^{68}Ga-FAPI PET/CT compared with standard-of-care imaging in patients with primary and recurrent PDAC.

MATERIALS AND METHODS

Patient Cohort

This cohort consisted of 19 patients with histologically confirmed PDAC. Written informed consent was obtained from all patients on an individual-patient basis following the regulations of the German Pharmaceuticals Act §13(2b). All patients were referred for the experimental diagnostics by their treating oncologists to assist diagnostic decision making. For example, in cases in which the results of standard imaging were inconclusive, more information was sought on tumor extension and possible involvement of regional lymph nodes for target-volume segmentation before radiotherapy, or there was a need to select target-positive patients for experimental last-line therapy with therapeutic FAPI conjugates. Clinical characteristics and outcomes were collected through electronic patient records. This retrospective study was approved by the local institutional review board (study number S-115/2020).

CT Imaging and Transabdominal Ultrasonography

All patients underwent multiphase ceCT imaging for staging. CT scans were acquire on average 17.6 d before FAP-specific PET/CT. Patients in a preoperative setting underwent additional transabdominal ultrasonography.

Radiopharmaceuticals and ^{68}Ga-FAPI PET/CT Imaging

Synthesis and labeling of both ^{68}Ga-FAPI-4 and ^{68}Ga-FAPI-46 followed the methods described by Lindner et al. (*25*) and Loktev et al. (*26*). A Biograph mCT Flow scanner (Siemens) was used for PET imaging. Scans were obtained according to scan protocols as previously published (*27,28*). In brief, after low-dose CT without contrast, PET scans were acquired in 3-dimensional mode (matrix, 200 × 200), emission data were corrected for attenuation, and reconstructions were performed. The injected activity for the ^{68}Ga-FAPI examinations ranged from 167 to 293 MBq.

For all patients, PET scans were obtained 1 h after injection of the radiotracer. This time point of image acquisition has been shown to be suitable for tumor imaging as we have observed high tumor-to-background ratios for various tumor entities including pancreatic carcinomas in our previous studies with FAPI PET (*25,27,*28,30).

To characterize ^{68}Ga FAPI uptake over time, multiple-time-point imaging was performed in 6 patients (the other patients did not undergo imaging at multiple imaging time points due to reduced general condition or limited compliance or limited imaging capacities).

Image Evaluation

The tracer biodistribution in patients was quantified by mean and maximum SUVs (SUV_{mean} and SUV_{max}, as widely accepted standard parameters for quantification and clinical evaluation of PET imaging) at 1 h after injection. For SUV calculation, circular regions of interest were drawn around the tumors on transaxial slices and automatically adapted to a 3-dimensional volume of interest with e.soft software (Siemens) at a 60% isocontour. The normal organs were evaluated with a 1-cm diameter (for the small organs: thyroid, parotid gland, myocardium, oral mucosa, spinal cord) or 2-cm diameter (brain, muscle, liver, pancreas, spleen, kidney, fat, aortic lumen content, lung) sphere placed inside the organ parenchyma. ^{68}Ga-FAPI PET/CT scans were evaluated by 1 board-certified radiologist, 1 board-certified radiation oncologist, and 2 board-certified nuclear medicine physicians in consensus. ceCT imaging was interpreted by 2 board-certified radiologists in consensus without knowledge of ^{68}Ga-FAPI PET/CT results, thus establishing the pre–^{68}Ga-FAPI PET/CT staging. The staging was coded according to the eighth edition of the TNM classification of malignant tumors of the Union for International Cancer Control (*31*).

Changes in TNM stage, localization of metastases, and oncologic management were recorded for all patients. This was done by documenting stage/tumor localization and oncologic management based on ceCT and based on ^{68}Ga-FAPI imaging by 2 nuclear medicine physicians and 2 radiation oncologists. All findings and changes were interpreted in consensus. Changes of oncologic management (^{68}Ga-FAPI PET/CT–based vs. ceCT-based) were graded by the level of impact: fundamental changes with regard to alteration of treatment type or treatment intent and relevant changes within a treatment regime were classified as major and minor, respectively.

FAP Immunohistochemistry

In 5 of the patients examined by ^{68}Ga-FAPI PET/CT, sufficient material for immunohistochemistry was available. All specimens were from the archives of the Department of Pathology, Institute of Pathology, University Hospital Heidelberg, Heidelberg, Germany. The primary anti-FAP antibody used was ab207178 (EPR20021; Abcam) diluted 1:100. Immunohistochemistry was done on 0.5-μm-thick formalin-fixed, paraffin-embedded tissue sections mounted on Superfrost Plus slides (Thermo Scientific) followed by drying at 80°C for 10 min. Stainings were done on a Ventana BenchMark XT Immunostainer (Ventana Medical Systems). The slices were pretreated with cell conditioner 1 (pH 8) for 92 min, followed by incubation with the primary antibody at 37°C for 32 min. The incubation was followed by Ventana standard signal amplification, UltraWash, counterstaining with 1 drop of hematoxylin for 4 min, and 1 drop of bluing reagent for 4 min. For visualization, the ultraView Universal DAB Detection Kit (Ventana Medical Systems) was used. Negative controls were obtained by omitting the primary antibody (data not shown). Images were scanned and digitalized using NanoZoomer S60 Digital slide scanner (Hamamatsu Photonics).

Statistical Analysis

We performed descriptive analyses for patients and their tumor characteristics. For determination of SUVs, median and range were used. The correlation of FAPI uptake within or outside the tumor was determined using a 2-sided t test; a P value of less than 0.05 was defined as statistically significant. All statistical analyses were performed using Microsoft Excel 2010.

TABLE 1
Clinical Data of 19 Patients with PDAC Examined by ^{68}Ga-FAPI PET/CT

Patient	Age (y)	Sex	Previous surgery	Previous chemotherapy	Previous radiation	Clinical indication	FAPI variant	Acquisition time (min after injection)
1	52	M	Whipple	FOLFIRINOX	Mediastinal lymph nodes	Recurrence/PD	FAPI-4	60
2	52	M	Whipple	No	No	Recurrence/PD	FAPI-4	60
3	52	F	No	FOLFIRINOX	No	Recurrence/PD	FAPI-46	10/60/180
4	58	M	Total pancreatectomy	FOLFIRINOX	No	Recurrence/PD	FAPI-4	60
5	58	M	no	No	No	Primary staging	FAPI-4	60
6	59	F	Distal pancreatectomy	Gem	No	Recurrence/PD	FAPI-46	10/60/180
7	60	M	No	FOLFIRINOX	No	Recurrence/PD	FAPI-4	60
8	60	M	No	No	No	Primary staging	FAPI-4	60
9	61	F	Whipple	Gem + Cap	No	Primary staging	FAPI-4	60
10	64	F	Whipple	FOLFIRINOX	No	Recurrence/PD	FAPI-4	60
11	64	M	Distal pancreatectomy	FOLFIRINOX	No	Recurrence/PD	FAPI-4	60
12	65	F	Whipple	FOLFIRINOX	No	Primary staging	FAPI-4	60
13	66	F	no	Gem	no	Primary Staging	FAPI-4	60
14	67	F	Distal pancreatectomy	FOLFIRINOX	No	Recurrence/PD	FAPI-4	60
15	68	F	No	No	No	Primary staging	FAPI-4	60
16	74	M	pp-Whipple	Cap + Ox	No	Recurrence/PD	FAPI-4	60
17	76	F	pp-Whipple	Gem + nab-paclitaxel	No	Recurrence/PD	FAPI-4	60/180
18	79	M	No	No	No	Primary staging	FAPI-4	60
19	80	M	No	Gem + nab-paclitaxel	Primary tumor	Recurrence/PD	FAPI-46	10/60/180

FOLFIRINOX = 5-fluorouracil, leukovorin, irinotecan, and oxaliplatin; Gem = gemcitabine; Cap = capecitabine; Ox = oxaliplatin; pp-Whipple: pylorus-preserving Whipple procedure.

RESULTS

Patient Cohort

Table 1 depicts the demographic data as well as the previous therapies of all 19 patients. Median patient age was 64.0 y (range, 52–80 y). Seven patients underwent FAP-specific PET/CT preoperatively as initial staging (4 of them were treatment-naïve, 3 of them had undergone neoadjuvant chemotherapy), 11 patients presented with local tumor recurrence, and 1 patient experienced progressive disease after neoadjuvant chemotherapy.

Biodistribution of ^{68}Ga-FAPI Tracers

One hour after injection, overall SUV_{max} and SUV_{mean} for all PDAC were 13.37 ± 5.45 and 7.32 ± 3.13, whereas preoperative tumors showed higher SUV_{max} and SUV_{mean} (17.41 ± 7.40 and 10.25 ± 4.10, respectively) than local recurrences (11.90 ± 3.31 and 6.34 ± 2.02, respectively). Similarly, elevated SUV_{max} and SUV_{mean} were observed in lymph node metastases (14.13 ± 8.50 and 7.62 ± 3.69, respectively) and distant metastases (7.34 ± 2.48 and 3.92 ± 1.57, respectively). All normal organs, including the uninvolved pancreas, showed low ^{68}Ga-FAPI uptake, which resulted in high tumor-to background ratios (e.g., SUV_{max} tumor to blood pool, 8.31; SUV_{max} tumor to muscle, 8.72; and SUV_{max} tumor to fat, 23.34). Figure 1 provides an overview of the biodistribution of tumor uptake in PDAC manifestations and the background activity of normal organs. Of note, both tracer variants (^{68}Ga-FAPI-4 and ^{68}Ga-FAPI-46) showed a similar biodistribution (Supplemental Fig. 1; supplemental materials are available at http://jnm.snmjournals.org).

Changes in TNM Staging and Oncologic Management After ^{68}Ga-FAPI PET/CT ^{68}Ga-FAPI PET/CT resulted in new findings in 10 of 19 patients, specifically; 8 of 12 patients with recurrent/

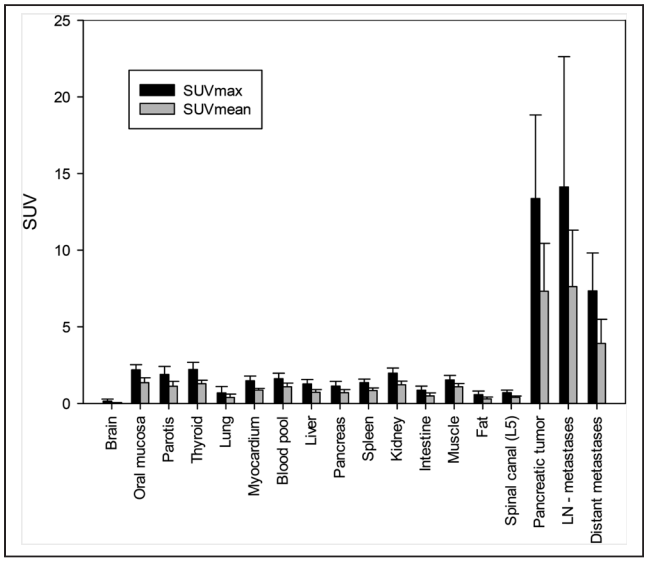

FIGURE 1. Biodistribution analysis (SUV_{max} and SUV_{mean}) of 19 patients with PDAC based on PET/CT imaging 1 h after injection of ^{68}Ga-labeled FAPI tracer molecules (FAPI-4 in 16 patients and FAPI-46 in 3 patients).

progressive disease were upstaged and 1 of 12 patients downstaged (Table 2). In patients with primary disease, 1 of 7 patients was upstaged and no patients were downstaged. In all cases, changes in staging were caused by the detection of new or additional distant metastases in one or more organ systems. Moreover, for 2 patients, there was a detection of new lymph node metastases. ^{68}Ga-FAPI PET/CT led to an upstaging to stage IV disease by detection of progression to distant metastatic disease in 1 of 7 and 3 of 12 patients with newly diagnosed or recurrent PDAC, respectively. In 1 patient with local recurrence, the lymph node status could not be evaluated definitely based on ceCT. Here, the absence of FAPI-positive lymph nodes led to more certainty.

Furthermore, in 1 patient ^{68}Ga-FAPI PET/CT led to downstaging. This patient had undergone a Whipple operation followed by FOLFIRINOX (5-fluorouracil, leukovorin, irinotecan, and oxaliplatin) chemotherapy. During follow-up, the patient was classified as having local recurrence by CT imaging (T2). Additional ^{68}Ga-FAPI PET/CT revealed no suspicious FAPI uptake (T0). On the basis of these results, the planned oncologic treatment for this patient was reassessed and a decision was made for watchful waiting instead of an initially considered local radiotherapy.

Figure 2 shows a case in which ^{68}Ga-FAPI PET/CT markedly changed primary TNM staging (upstaging) compared with ceCT and ^{18}F-FDG PET/CT. Figure 3 shows an exemplary case of upstaging after ^{68}Ga-FAPI PET/CT compared with ceCT in the setting of local recurrence. Hybrid imaging caused changes in oncologic management in 7 patients. Although minor changes occurred in 2 patients, 5 patients had major changes including cancellation of the planned therapy and watchful waiting instead (1 patient), cancelling of the planned pancreatectomy after confirmation of a FAPI-positive pulmonary metastasis by biopsy (1 patient, Fig. 2), local irradiation of a single hepatic lesion (1 patient), and FAPI ligand therapy on an individual-patient basis (2 patients). Four patients with recurrent or progressive PDAC

TABLE 2
Comparison of ceCT-Based and ^{68}Ga-FAPI PET/CT–Based TNM Staging of 19 Patients with Primary and Recurrent/Progressive PDAC

Patient	Clinical indication	TNM stage (CT-based)	TNM stage (FAPI PET–based)	Additional finding in FAPI PET	Staging change
1	Relapse/progression	T1 N2 M1 (LYM, PUL)	T1 N0 M1 (LYM)	(Recurrent) mediastinal lymph node metastases	Up
2	Relapse/progression	T4 N0 M1 (PER)	T4 N0 M1 (PER)	None	None
3	Relapse/progression	T3 N0 M0	T3 N0 M1 (OSS)	Bone metastasis	Up
4	Relapse/progression	T4 N0 Mx	T4 N0 M1 (PER)	Peritoneal carcinosis	Up
5	Primary staging	T1 N0 M0	T1 N0 M0	None	None
6	Relapse/progression	T3 N0 M0	T3 N0 M0	None	None
7	Relapse/progression	T4 N0 Mx	T4 N0 M0	None	None
8	Primary staging	T4 N0 Mx	T4 N0 M0	None	None
9	Primary staging	T4 N0 M0	T4 N0 M0	None	None
10	Relapse/progression	T2 N0 M0	T0 N0 M0	No local recurrence (T0)	Down
11	Relapse/progression	T4 N0 M1 (LYM, HEP)	T4 N2 M1 (LYM, HEP, OSS)	Abdominal lymph node metastases, 2 more liver metastases, bone metastasis	Up
12	Primary staging	T4 N0 Mx	T4 N0 M0	None	None
13	Primary staging	T3 N0 M0	T3 N0 M0	None	None
14	Relapse/progression	T4 N2 M1 (HEP)	T4 N2 M1 (HEP, PER)	Peritoneal carcinosis	Up
15	Primary staging	T4 N2 Mx	T4 N2 M1 (PER, PLE)	Pleural carcinosis, peritoneal carcinosis, liver metastases	Up
16	Relapse/progression	T0 N2 M1 (LYM, HEP)	T0 N2 M1 (LYM, HEP, OSS)	Bone metastasis	Up
17	Relapse/progression	T2 N0 Mx	T2 N0 M1 (HEP, PUL)	Liver metastases without CT correlate, pulmonary metastasis	Up
18	Primary staging	T1 N0 Mx	T1 N0 M0	None	None
19	Relapse/progression	T4 Nx M1 (PER)	T4 N1 M1 (PER, OSS, HEP)	Lymph nodes definable from tumor conglomerate, bone metastases, liver metastases	Up

LYM = lymphatic; PUL = pulmonary; PER = peritoneal; HEP = hepatic; PLE = pleural.

were selected for radiotherapy, and the ^{68}Ga-FAPI PET/CT data were used for target volume delineation.

^{68}Ga-FAPI Uptake of PDAC and Pancreatitis

Eleven of 19 patients had undergone no or only partial pancreatectomy before ^{68}Ga-FAPI PET/CT. In 8 of these patients, significantly elevated tracer uptake was observed not only in the PDAC, but also homogeneously within the rest of the pancreas. Four of these patients had been diagnosed with chronic pancreatitis before ^{68}Ga-FAPI PET/CT imaging. As tumor-related buildup of exocrine secretions and consequent pancreatitis is a typical finding in PDAC, we assumed that the patients without prediagnosed chronic pancreatitis were experiencing tumor-related pancreatitis. We considered pancreatic ^{68}Ga-FAPI uptake as a sign of pancreatitis in all 8 patients.

Although tumors showed higher average SUV_{max} and SUV_{mean} (15.64 ± 5.81 and 8.65 ± 3.61, respectively) than pancreatitis (7.50 ± 3.52 and 4.07 ± 2.11, respectively) after 1 h, we observed a certain overlap between tumor-related and inflammatory uptake, as illustrated by the box plot graphs in Figures 4A and 4B. In 1 patient with PDAC and pancreatitis, we performed ^{68}Ga-FAPI PET/CT after 10, 60, and 180 min. Here, we observed slightly increasing uptake of the PDAC (SUV_{max} 11.48, 12.66, and 13.23 and SUV_{mean} 6.65, 7.46, and 7.71, respectively, after 10, 60, and 180 min) and decreasing uptake within the pancreatitis in the remaining pancreas (SUV_{max} 7.24, 6.55, and 5.63 and SUV_{mean} 4.32, 3.01, and 2.96, respectively, after 10, 60, and 180 min). Figure 4C shows exemplary images of PDAC and pancreatitis-related FAPI uptake over time for this patient. Another patient with both PDAC and pancreatitis who underwent imaging after 60 and 180 min showed similar uptake kinetics (tumor: SUV_{max} 12.05 and 12.43 and SUV_{mean} 7.37 and 7.74, respectively, after 60 and 180 min and pancreatitis: SUV_{max} 6.12 and 5.56 and SUV_{mean} 3.28 and 2.77, respectively, after 60 and 180 min).

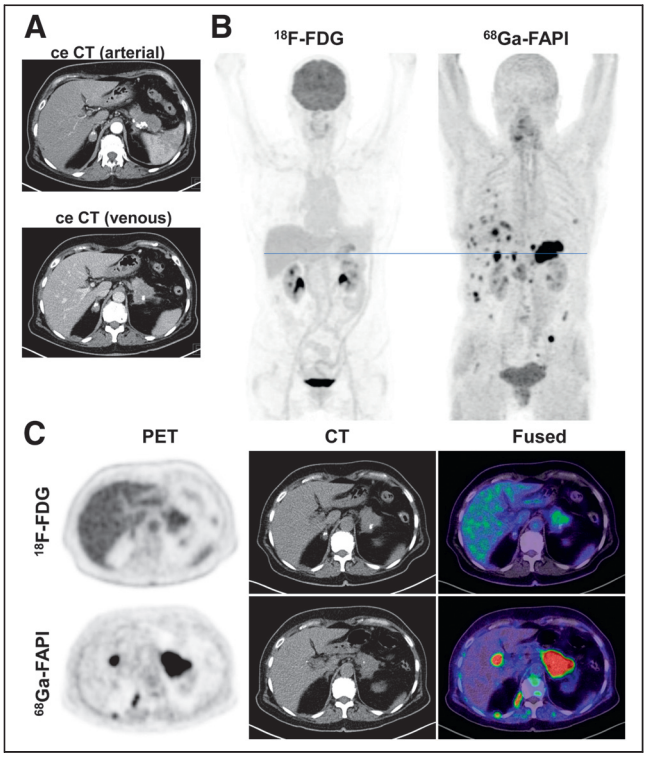

FIGURE 2. Primary staging of a patient with PDAC. (A) Axial images of PDAC and liver in arterial (upper image) and venous (lower image) ceCT scan. (B) Mean intensity projection (MIP) images of ^{18}F-FDG and FAPI PET/CT imaging. (C) Axial ^{18}F-FDG and FAPI PET/CT images of same patient on level (blue line in A) of pancreatic tumor mass and another suspicious FAPI accumulation in projection on perihepatic lymph node. Metastatic situation, which had been revealed by FAPI PET/CT, was confirmed by biopsy of pulmonary lesion that was diagnosed as metastasis of known PDAC.

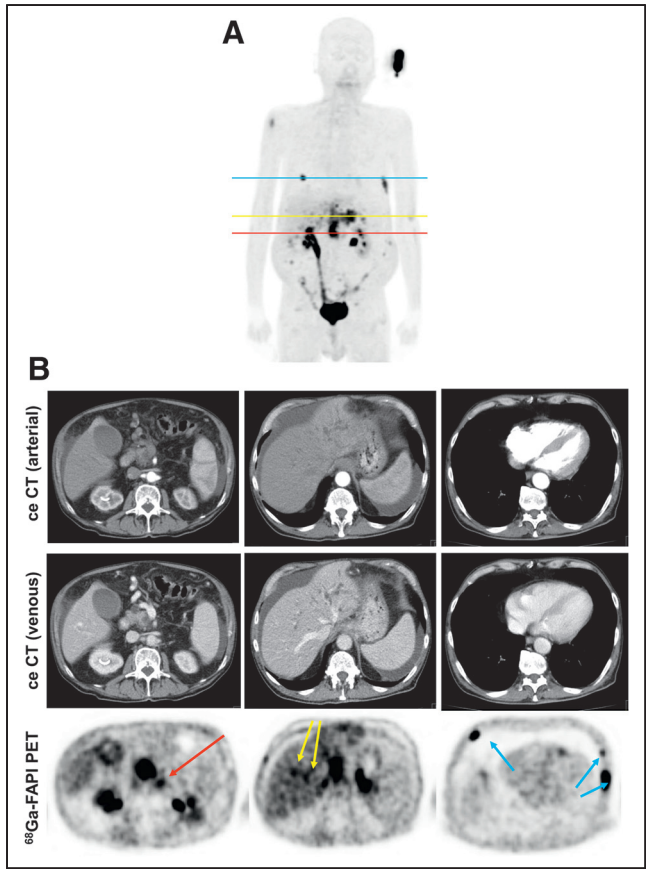

FIGURE 3. Staging of patient with local recurrence of PDAC. (A) Mean intensity projection (MIP) image of FAPI PET/CT imaging. (B) Axial ceCT and FAPI PET/CT images of same patient on level of local recurrence (red line in A), 2 metastasis-suspicious intrahepatic foci (yellow line in A), and 3 suspicious osseous tracer accumulations (blue line in A). In contrast to CT imaging, FAPI PET/CT allows discrimination of metastatic lymph node from local recurrence mass (red arrow). FAPI PET/CT also revealed possible new liver (yellow arrows) and bone (blue arrows) metastases.

The other 4 patients with imaging at more than one imaging time point had a local recurrence after pancreatectomy. Thus, we could evaluate only tumor lesions in these patients. Tumor lesions of all 6 patients with more than one imaging time point showed stable uptake between 10 and 60 min and a slight tendency to decreased uptake after 180 min. Figure 4D shows the summed SUV_{max} and SUV_{mean} in the PDAC lesions of all patients who underwent imaging at more than one time point.

^{68}Ga-FAPI Uptake Related in Other Chronic Inflammatory and Reactive Processes

Next to pancreatitis-related FAPI uptake, we regularly found moderately elevated FAPI uptake related to chronic inflammatory or reactive processes in other body sites, namely joint-associated,

arthrosis-related uptake (10 patients), in postoperative scars (2 patients), located in the mamma (1 patient, most likely due to mastitis), around a γ-nail implant (1 patient), and related to tendinopathy (1 patient).

FAP Expression in Pancreatic Carcinomas

To further characterize FAP as a target structure within pancreatic carcinomas, we performed FAP immunohistochemistry in 4 of the patients included. Supplemental Figure 2 shows hematoxylin and eosin staining and FAP immunohistochemistry of 2 exemplary PDAC. For the first PDAC, Supplemental Figures 2A–2D show strong FAP expression in the tumor stroma, whereas the neoplastic cells were FAP-negative. The stroma of the second PDAC (Supplemental Figures 2E–2H) was also FAP-positive, but less intensively. In this case, we observed FAP-positive cell clusters within the neoplastic cells, whereas FAP positivity was pronounced in the peripheral zone of the cell clusters. These FAP-positive cell clusters most likely represent Langerhans islets, as it has been shown that the α-cells of Langerhans islets express FAP (*32*).

DISCUSSION

This retrospective analysis of 19 patients with PDAC suggests that ^{68}Ga-FAPI PET/CT is a promising new imaging modality in staging of PDAC that may help to detect new or clarify inconclusive results obtained by standard CT imaging. Analyses of tracer biodistribution demonstrated a high FAPI uptake in primary PDAC as well as lymph nodes and distant metastases, whereas healthy tissues have negligible background activity, leading to excellent tumor-to-background ratios for PDAC, similar to those shown by previous studies on FAPI PET/CT in PDAC and other tumors (*27–29,33*).

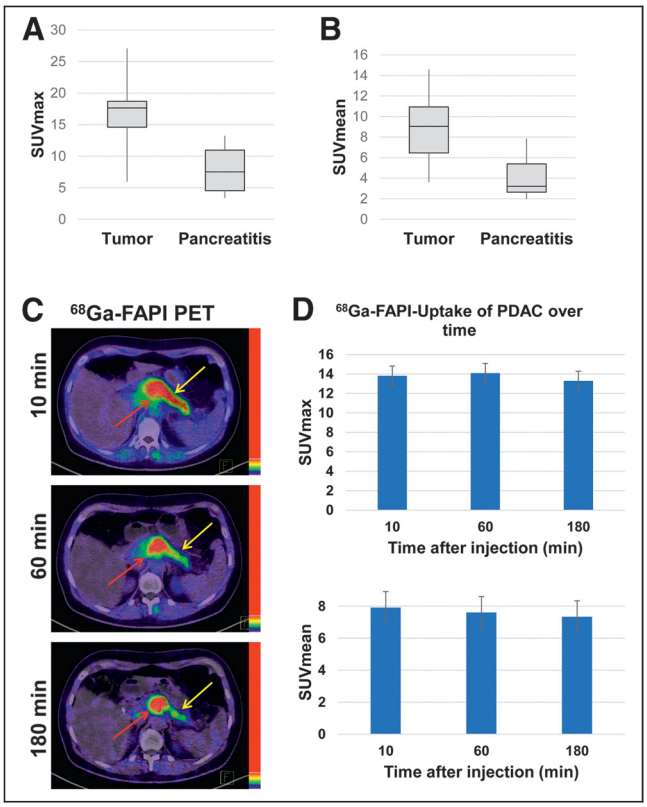

FIGURE 4. (A and B) Average SUV_{max} and SUV_{mean} 1 h after injection of ^{68}Ga-labeled FAPI tracers in 8 PDAC and in accompanying pancreatitis in rest of pancreas. (C) Exemplary images of tumor-related (red arrow) and pancreatitis-related (yellow arrow) ^{68}Ga-FAPI uptake 10, 60, and 180 min after application. (D) ^{68}Ga-FAPI uptake 10, 60, and 180 min after application (SUV_{max} and SUV_{mean} values) in PDAC lesions of 6 patients.

PDAC is clinically challenging with very high mortality rates. Improvement in survival can only be achieved by effective treatment approaches customized to the individual patient's disease status. Thus, hybrid imaging using FAPI tracer may open up new applications in staging and restaging of PDAC. To evaluate the potential impact of ^{68}Ga-FAPI PET/CT on the clinical management of PDAC, we have documented that ^{68}Ga-FAPI PET/CT resulted in changes of TNM staging of primary and recurrent/progressive PDAC compared with standard-of-care imaging. Clinically meaningful changes in TNM staging in a high percentage of recurrent tumors (9/12 cases) was seen and resulted in therapy changes. In staging for newly diagnosed PDAC upstaging occurred in 1 of 7 cases. These changes in TNM classification had a significant impact on oncologic management. Apart from changes concerning systemic therapy, the use of ^{68}Ga-FAPI PET/CT may also help to select patients for local treatment approaches such as surgery or radiotherapy. In fact, 4 patients were considered candidates for irradiation according to standard staging. For all these patients, the ^{68}Ga-FAPI PET/CT data were used for radiotherapy planning. Radiotherapy was conducted as a local treatment approach for unresectable disease, recurrent disease, and in the setting of oligometastatic lymph nodes with either photons or carbon ions. For the management of local recurrences or unresectable PDAC, the application of carbon ions is considered a promising radiotherapeutic modality (*34*).

FAPI PET/CT may lead to significant changes in oncologic management when compared with ^{18}F-FDG PET/CT. A recent study with head-to-head comparison of ^{18}F-FDG PET/CT and FAPI PET/CT in various tumors showed a tendency toward upstaging after FAPI PET for 4 pancreatic carcinomas (*29*). On the basis of our comparison of FAPI PET/CT and ceCT, we speculate that there may be a similar discrepancy between ^{18}F-FDG PET/CT and FAPI PET/CT–based staging and resulting treatment decisions for PDAC. A study addressing this specific question in PDAC would be an important contribution.

With respect to the discrimination of PDAC and pancreatitis, it must be emphasized that we have observed higher FAPI uptake in PDAC than in pancreatitis. However, there seems to be an overlap of the uptake intensities on static imaging after 1 h. Repeated imaging in 2 patients indicated that there may be differential uptake kinetics in PDAC (slightly increasing tracer uptake over time) and pancreatitis or fibrotic pancreatic tissue (decreasing tracer uptake over time). These findings are similar to our observations of dynamic FAPI PET/CT in patients with pulmonary fibrosis and lung cancer (Röhrich et al., unpublished data, July 2018 to August 2019). However, the results of the current study regarding the differential FAPI uptake over time in PDAC and pancreatitis can be considered only preliminary. The hypothesis of differential uptake over time in PDAC and pancreatitis should be evaluated systematically in a larger patient cohort. Also, dynamic FAPI PET imaging may provide useful additional parameters for this question.

The major limitation of this study is the relatively low number of patients, which does not allow us to draw any definite conclusions on the diagnostic value of ^{68}Ga-FAPI PET/CT. However, the high uptake values in PDAC suggest this will be a highly sensitive modality especially in recurrent and progressive disease.

The results regarding the tracer biodistribution and the impact on TNM staging are promising and show great clinical potential for the future application of ^{68}Ga-FAPI PET/CT for decision making on appropriate treatment options in PDAC. Moreover as serum screening methods become available for early PDAC detection, FAPI PET/CT is a potential method of detecting these early tumors. Implementation of ^{68}Ga-FAPI PET/CT in further clinical studies is recommended to gain further evidence of the value of this new imaging modality. In our exemplary histologic studies, we observed strong stromal FAP expression in 4 primary PDAC. Systematic ^{68}Ga-FAPI PET–based bioptic studies of primary and metastatic lesions are needed to gain more diagnostic certainty regarding tumor-related FAPI uptake in PDAC and other malignancies.

Another limitation is that 2 different tracer molecules (FAPI-4 and FAPI-46) were used in this study. Molecules were switched during the investigation period of this study because FAPI-46 may open a theranostic perspective due to improved long-time tumor retention and tumor-to organ ratios. For our analysis, this switch of molecules was a minor limitation because it has been shown that both substances do not significantly differ in their radiopharmaceutical properties at early time points (1–4 h) (*30*), which we confirmed for this dataset by separate biodistribution analysis of both tracer molecules.

CONCLUSION

FAPI PET/CT is a promising imaging modality for PDAC, with high tracer uptake and excellent tumor-to-background ratios. FAPI PET/CT–based TNM staging differed in about half of all patients and nearly all patients with recurrent disease compared with staging obtained by ceCT. In the primary setting, dynamic FAPI PET/CT imaging may be helpful for the discrimination of tumor versus inflammatory or fibrotic pancreatic lesions. The clinical value of FAPI PET/CT should be further investigated.

DISCLOSURE

This work was funded by the Federal Ministry of Education and Research, grant number 13N 13341. Uwe Haberkorn, Clemens Kratochwil and Frederik Giesel have filed a patent application for quinoline-based FAP-targeting agents for imaging and therapy in nuclear medicine. This retrospective study was approved by the local institutional review board (study number S-115/2020). No other potential conflict of interest relevant to this article was reported.

KEY POINTS

QUESTION: Does ^{68}Ga-FAPI PET/CT impact TNM staging and clinical management of PDAC?

PERTINENT FINDINGS: FAPI PET/CT led to significant changes in staging and clinical management of 19 patients with PDAC compared with ceCT, especially in the setting of local recurrence.

IMPLICATIONS FOR PATIENT CARE: On the basis of the encouraging results of this analysis, the clinical value FAPI PET/CT in primary and recurrent PDAC should be further validated. FAPI PET may be implemented in the future clinical management of PDAC patients.

REFERENCES

1. Siegel RL, Miller KD, Jemal A. Cancer statistics, 2019. *CA Cancer J Clin*. 2019;69:7–34.
2. Conrad C, Fernandez-Del Castillo C. Preoperative evaluation and management of the pancreatic head mass. *J Surg Oncol*. 2013;107:23–32.
3. Montejo Gañán I, Angel Rios LF, Sarria Octavio de Toledo L, Martinez Mombila ME, Ros Mendoza LH. Staging pancreatic carcinoma by computed tomography. *Radiologia*. 2018;60:10–23.
4. Bowman AW, Bolan CW. MRI evaluation of pancreatic ductal adenocarcinoma: diagnosis, mimics, and staging. *Abdom Radiol (NY)*. 2019;44:936–949.
5. Alabousi M, McInnes MD, Salameh JP, et al. MRI vs. CT for the detection of liver metastases in patients with pancreatic carcinoma: a comparative diagnostic test accuracy systematic review and meta-analysis. *J Magn Reson Imaging*. 2021;53:38–48.
6. Kitano M, Yoshida T, Itonaga M, Tamura T, Hatamaru K, Yamashita Y. Impact of endoscopic ultrasonography on diagnosis of pancreatic cancer. *J Gastroenterol*. 2019;54:19–32.
7. Zins M, Matos C, Cassinotto C. Pancreatic adenocarcinoma staging in the era of preoperative chemotherapy and radiation therapy. *Radiology*. 2018;287:374–390.
8. Qayyum A, Tamm EP, Kamel IR, et al. ACR appropriateness criteria® staging of pancreatic ductal adenocarcinoma. *J Am Coll Radiol*. 2017;14:S560–S569.
9. Yeh R, Dercle L, Garg I, Wang ZJ, Hough DM, Goenka AH. The role of ^{18}F-FDG PET/CT and PET/MRI in pancreatic ductal adenocarcinoma. *Abdom Radiol (NY)*. 2018;43:415–434.
10. Yoshioka M, Sato T, Furuya T, et al. Role of positron emission tomography with 2-deoxy-2-[^{18}F]fluoro-D-glucose in evaluating the effects of arterial infusion chemotherapy and radiotherapy on pancreatic cancer. *J Gastroenterol*. 2004;39:50–55.
11. Sperti C, Pasquali C, Bissoli S, Chierichetti F, Liessi G, Pedrazzoli S. Tumor relapse after pancreatic cancer resection is detected earlier by 18-FDG PET than by CT. *J Gastrointest Surg*. 2010;14:131–140.
12. Wang L, Dong P, Shen G, et al. ^{18}F-fluorodeoxyglucose positron emission tomography predicts treatment efficacy and clinical outcome for patients with pancreatic carcinoma: a meta- analysis. *Pancreas*. 2019;48:996–1002.
13. Kauhanen SP, Komar G, Seppanen MP, et al. A prospective diagnostic accuracy study of ^{18}F-fluorodeoxyglucose positron emission tomography/computed tomography, multidetector row computed tomography, and magnetic resonance imaging in primary diagnosis and staging of pancreatic cancer. *Ann Surg*. 2009;250:957–963.
14. Strobel O, Buchler MW. Pancreatic cancer: FDG-PET is not useful in early pancreatic cancer diagnosis. *Nat Rev Gastroenterol Hepatol*. 2013;10:203–205.
15. Leppänen J, Lindholm V, Isohookana J, et al. Tenascin C, fibronectin, and tumor-stroma ratio in pancreatic ductal adenocarcinoma. *Pancreas*. 2019;48:43–48.
16. Spill F, Reynolds DS, Kamm RD, Zaman MH. Impact of the physical microenvironment on tumor progression and metastasis. *Curr Opin Biotechnol*. 2016;40:41–48.
17. Valkenburg KC, de Groot AE, Pienta KJ. Targeting the tumour stroma to improve cancer therapy. *Nat Rev Clin Oncol*. 2018;15:366–381.
18. von Ahrens D, Bhagat TD, Nagrath D, Maitra A, Verma A. The role of stromal cancer-associated fibroblasts in pancreatic cancer. *J Hematol Oncol*. 2017;10:76–83.
19. Nielsen MFB, Mortensen MB, Detlefsen S. Typing of pancreatic cancer-associated fibroblasts identifies different subpopulations. *World J Gastroenterol*. 2018;24:4663–4678.
20. Whittle MC, Hingorani SR. Fibroblasts in pancreatic ductal adenocarcinoma: biological mechanisms and therapeutic targets. *Gastroenterology*. 2019;156:2085–2096.
21. Sun Q, Zhang B, Hu Q, et al. The impact of cancer-associated fibroblasts on major hallmarks of pancreatic cancer. *Theranostics*. 2018;8:5072–5087.
22. Kalluri R. The biology and function of fibroblasts in cancer. *Nat Rev Cancer*. 2016;16:582–598.
23. Sahai E, Astsaturov I, Cukierman E, et al. A framework for advancing our understanding of cancer-associated fibroblasts. *Nat Rev Cancer*. 2020;20:174–186.
24. McCarthy JB, El-Ashry D, Turley EA. Hyaluronan, cancer-associated fibroblasts and the tumor microenvironment in malignant progression. *Front Cell Dev Biol*. 2018;6:48.
25. Lindner T, Loktev A, Altmann A, et al. Development of quinoline-based theranostic ligands for the targeting of fibroblast activation protein. *J Nucl Med*. 2018;59:1415–1422.
26. Loktev A, Lindner T, Mier W, et al. A tumor-imaging method targeting cancer-associated fibroblasts. *J Nucl Med*. 2018;59:1423–1429.
27. Kratochwil C, Flechsig P, Lindner T, et al. ^{68}Ga-FAPI PET/CT: tracer uptake in 28 different kinds of cancer. *J Nucl Med*. 2019;60:801–805.

28. Giesel FL, Kratochwil C, Lindner T, et al. ^{68}Ga-FAPI PET/CT: biodistribution and preliminary dosimetry estimate of 2 DOTA-containing FAP-targeting agents in patients with various cancers. *J Nucl Med*. 2019;60:386–392.
29. Chen H, Pang Y, Wu J, et al. Comparison of [^{68}Ga]Ga-DOTA-FAPI-04 and [^{18}F] FDG PET/CT for the diagnosis of primary and metastatic lesions in patients with various types of cancer. *Eur J Nucl Med Mol Imaging*. 2020;47:1820–1832.
30. Loktev A, Lindner T, Burger EM, et al. Development of fibroblast activation protein-targeted radiotracers with improved tumor retention. *J Nucl Med*. 2019;60: 1421–1429.
31. Kamarajah SK, Burns WR, Frankel TL, Cho CS, Nathan H. Validation of the American Joint Commission on Cancer (AJCC) 8th ed. staging system for patients with pancreatic adenocarcinoma: A Surveillance, Epidemiology and End Results (SEER) analysis. *Ann Surg Oncol*. 2017;24:2023–2030.
32. Busek P, Hrabal P, Fric P, Sedo A. Co-expression of the homologous proteases fibroblast activation protein and dipeptidyl peptidase-IV in the adult human Langerhans islets. *Histochem Cell Biol*. 2015;143:497–504.
33. Röhrich M, Loktev A, Wefers AK, et al. IDH-wildtype glioblastomas and grade III/IV IDH- mutant gliomas show elevated tracer uptake in fibroblast activation protein-specific PET/CT. *Eur J Nucl Med Mol Imaging*. 2019;46:2569–2580.
34. Liermann J, Shinoto M, Syed M, Debus J, Herfarth K, Naumann P. Carbon ion radiotherapy in pancreatic cancer: a review of clinical data. *Radiother Oncol*. 2020;147:145–150.